

Supporting Information

Copper Bispidines Complexes – Synthesis and Complex Stability Study

Aleksei V. Medved'ko, Bayirta V. Egorova, Alina A. Komarova, Rustem D. Rakhimov, Dmitry P. Krut'ko, Stepan N. Kalmykov, Sergey Z. Vatsadze

Contents

Titration curves for ligand 1c	S2
Titration curves for ligand 2a	S3
Titration curves for ligand 2c	S4
Titration curves for ligand 3b	S5
Titration curves for ligand 3c	S6
Stoichiometry of complex $\text{Cu}^{2+}:\mathbf{1c}$ determination by UV-vis spectrometry	S8
NMR spectra	S9
ATR-FTIR spectra of compounds 3b and 5b , 3c and 5c	S22
UV-vis spectrum of compound 4b	S23
HRMS-ESI of copper complexes 4b and 4c	S23
CV curves for complexes 4b and 5c	S24

Protonation of Ligand **1c**

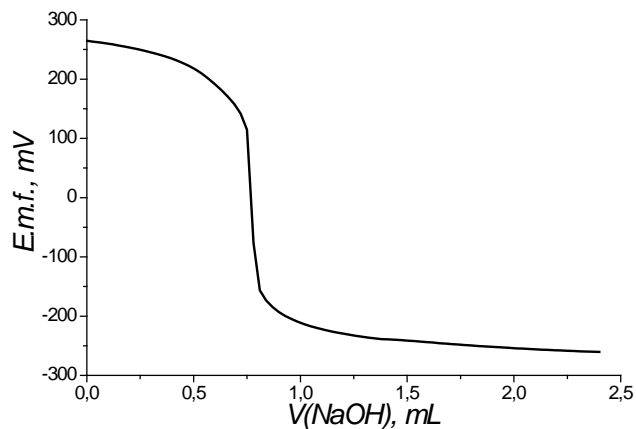


Figure S1. Titration curve of **1c** (0.001M) acidified by excess of HClO_4 (0.004M), $I=0.1 \text{ M KNO}_3$

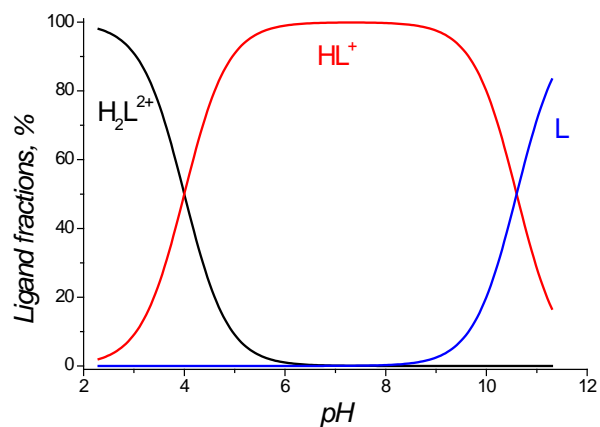


Figure S2. Species distribution for **1c** (0.001M), $I=0.1 \text{ M KNO}_3$

Complex of Ligand **1c** with Cu^{2+}

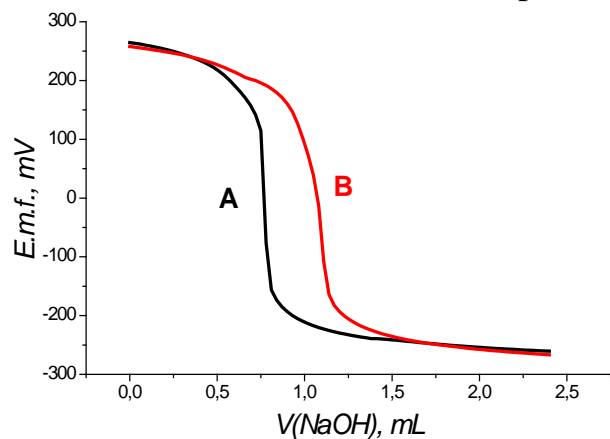


Figure S3. Titration curves: A- **1c** (0.001M) acidified by excess of HClO_4 (0.004M), B- **1a** (0.001M) with Cu^{2+} (0.0005M) acidified by excess of HClO_4 (0.004M), $I=0.1 \text{ M KNO}_3$

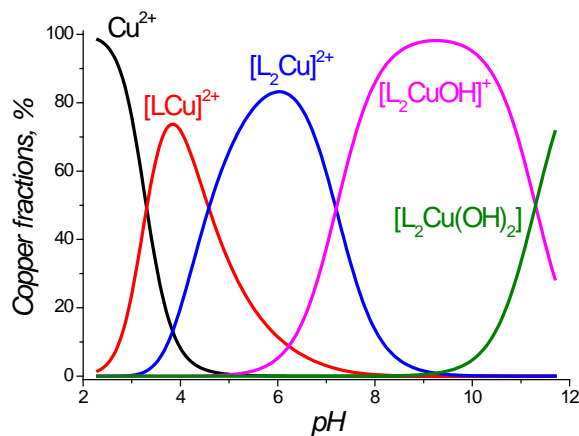


Figure S4. Species distribution in the system: **1c** (0.001M) and Cu^{2+} (0.0005M), $I=0.1 \text{ M KNO}_3$

Protonation of Ligand 2a

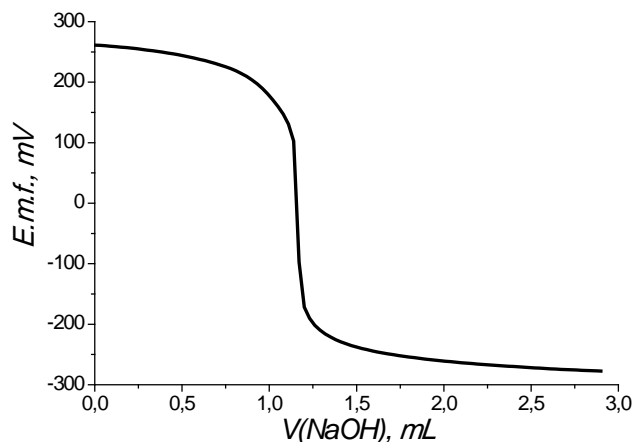


Figure S5. Titration curve of the **2a** (0.001M) acidified by excess of HClO_4 (0.004M), $I=0.1 \text{ M KNO}_3$

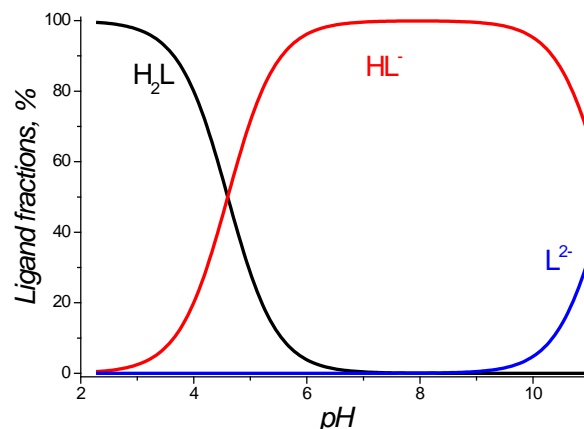


Figure S6. Species distribution for **2a** (0.001M), $I=0.1 \text{ M KNO}_3$

Complex of Ligand 2a with Cu^{2+}

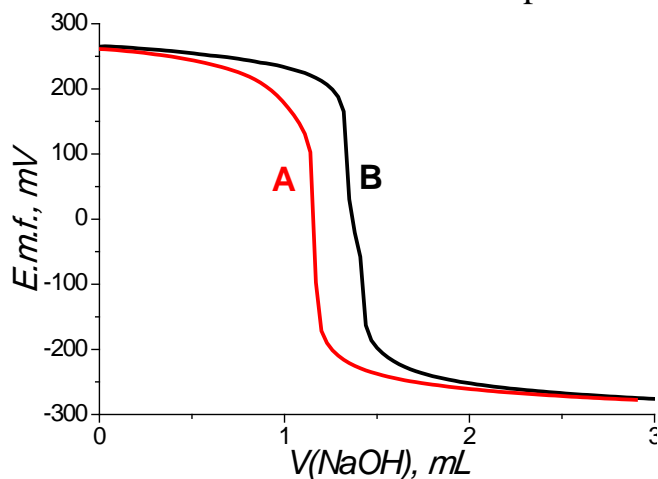


Figure S7. Titration curves of (A) the **2a** (0.001M) acidified by excess of HClO_4 (0.004M) and (B) the **2a** (0.001M) with Cu^{2+} (0.001M) acidified by excess of HClO_4 (0.004M), $I=0.1 \text{ M KNO}_3$

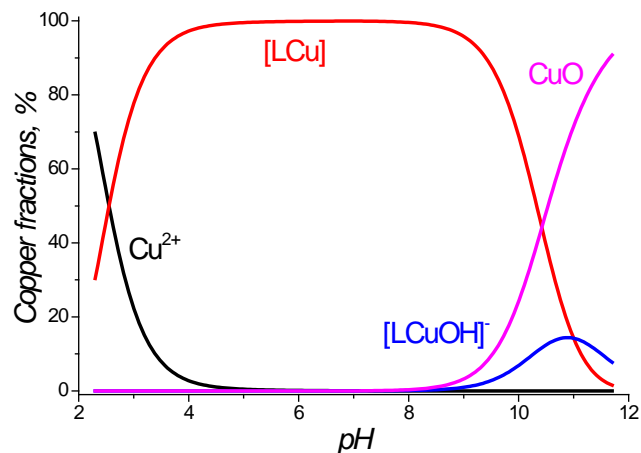


Figure S8. Species distribution in the system: **2a** (0.001M) and Cu^{2+} (0.001M), $I=0.1 \text{ M KNO}_3$

Protonation of Ligand **2c**

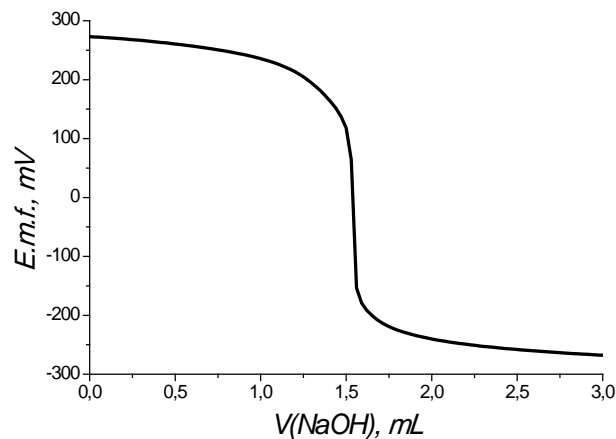


Figure S9. Titration curve of the **2c** (0.001M) acidified by excess of HClO_4 (0.004M), $I=0.1 \text{ M KNO}_3$

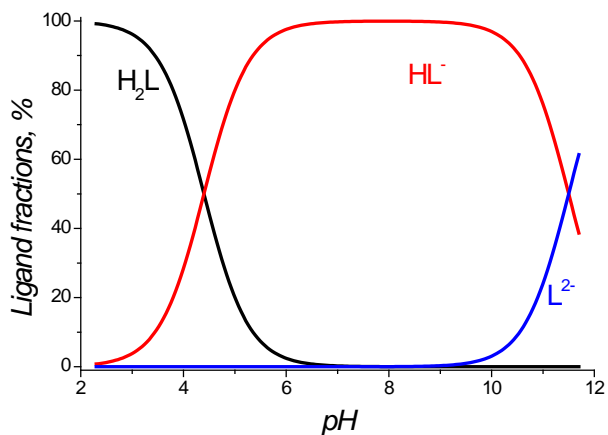


Figure S10. Species distribution for **2c** (0.001M), $I=0.1 \text{ M KNO}_3$

Complex of Ligand **2c** with Cu^{2+}

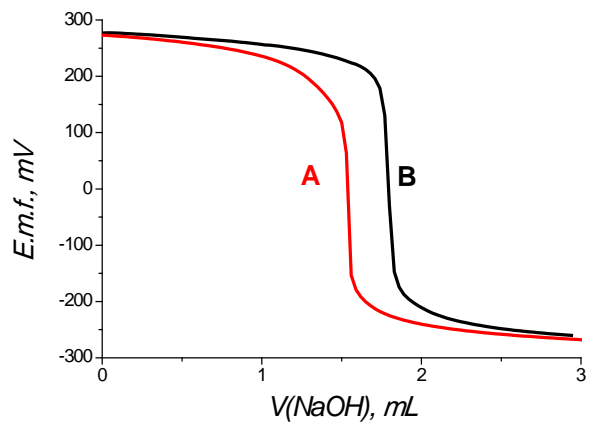


Figure S11. Titration curves of (A) the **2c** (0.001M) acidified by excess of HClO_4 (0.004M) and (B) the **2c** (0.001M) with Cu^{2+} (0.001M) acidified by excess of HClO_4 (0.004M), $I=0.1 \text{ M KNO}_3$

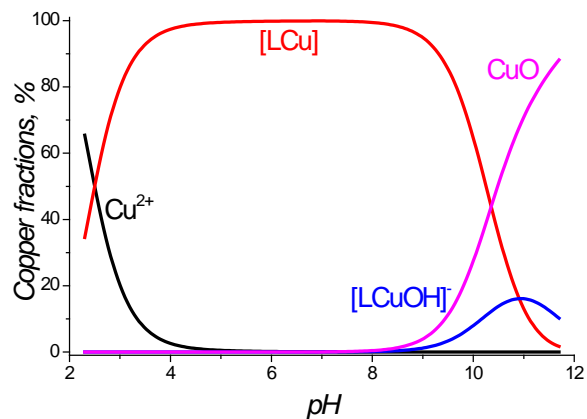


Figure S12. Species distribution curves in the system: **2c** (0.001M) and Cu^{2+} (0.001M), $I=0.1 \text{ M KNO}_3$

Protonation of Ligand **3b**

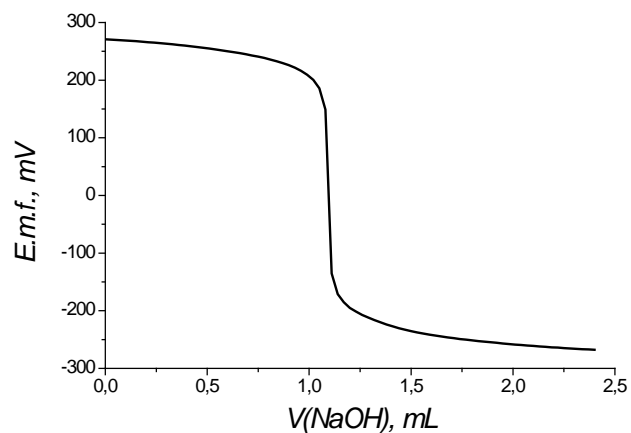


Figure S13. Titration curve of the **3b** (0.001M) acidified by excess of HClO_4 (0.004M), $I=0.1 \text{ M KNO}_3$

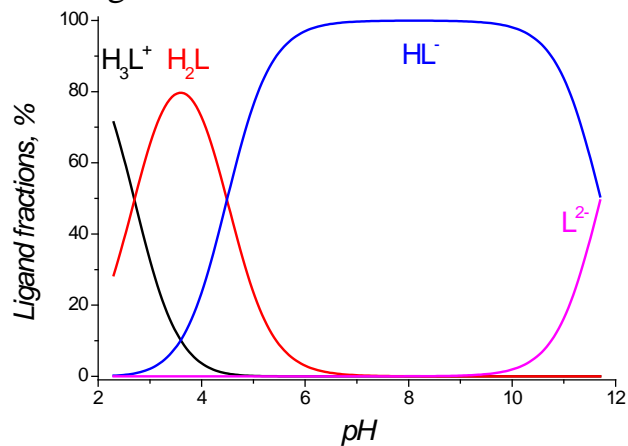


Figure S14. Species distribution for **3b** (0.001M), $I=0.1 \text{ M KNO}_3$

Complex of Ligand **3b** with Cu^{2+}

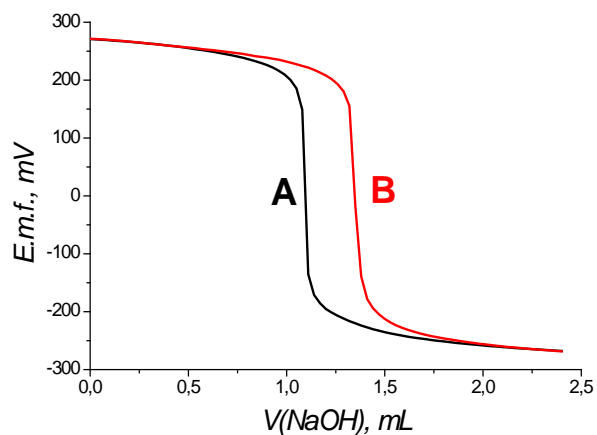


Figure S15. Titration curves of (A) the **3b** (0.001M) acidified by excess of HClO_4 (0.004M) and (B) the **3b** (0.001M) with Cu^{2+} (0.001M) acidified by excess of HClO_4 (0.004M), $I=0.1 \text{ M KNO}_3$

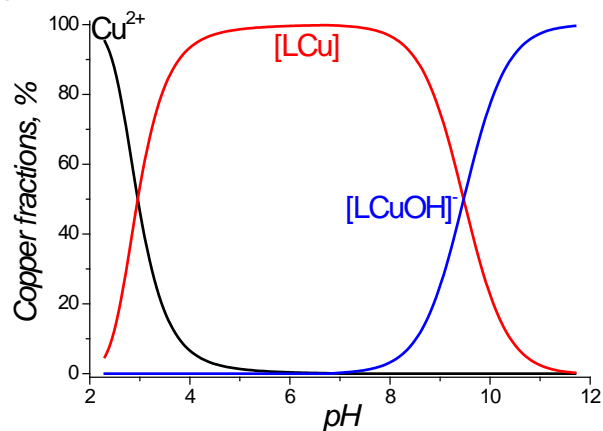


Figure S16. Species distribution curves in the system: **3b** (0.001M) and Cu^{2+} (0.001M), $I=0.1 \text{ M KNO}_3$

Protonation of Ligand 3c

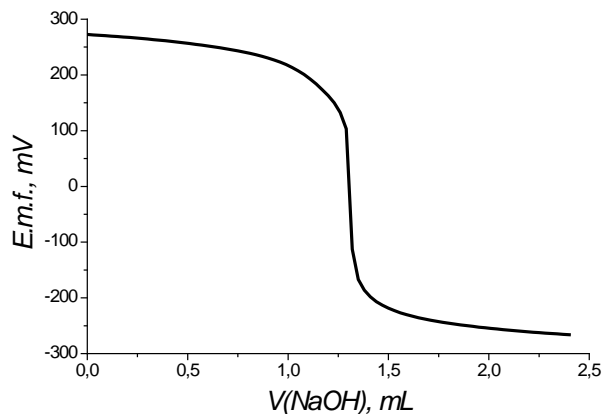


Figure S17. Titration curve of the **3c** (0.001M) acidified by excess of HClO_4 (0.004M), $I=0.1 \text{ M KNO}_3$

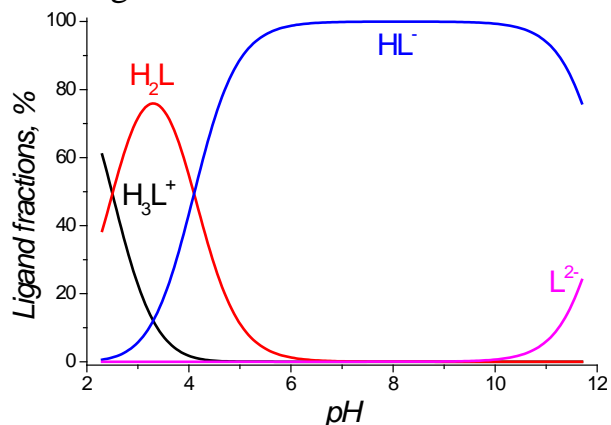


Figure S18. Species distribution for **3c** (0.001M), $I=0.1 \text{ M KNO}_3$

Complex of Ligand 3c with Cu^{2+}

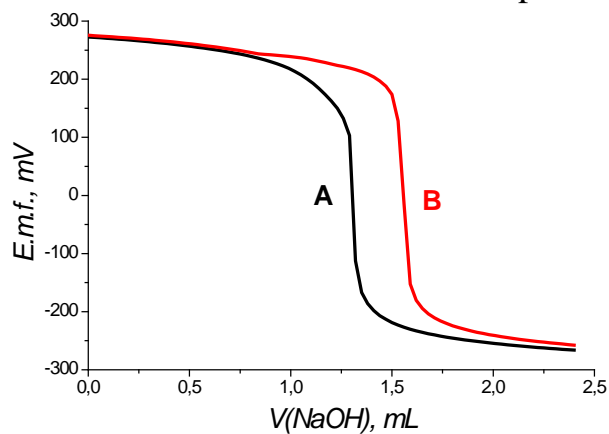


Figure S19. Titration curves of (A) the **3c** (0.001M) acidified by excess of HClO_4 (0.004M) and (B) the **3c** (0.001M) with Cu^{2+} (0.001M) acidified by excess of HClO_4 (0.004M), $I=0.1 \text{ M KNO}_3$

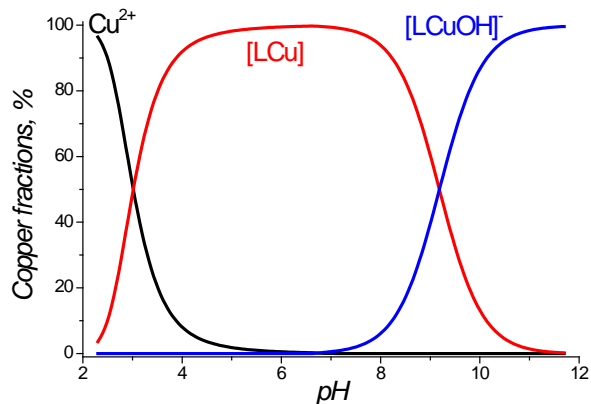


Figure S20. Species distribution curves in the system: **3c** (0.001M) and Cu^{2+} (0.001M), $I=0.1 \text{ M KNO}_3$

Stoichiometry of complex $\text{Cu}^{2+}:\mathbf{1c}$: determination by UV-vis spectrophotometry

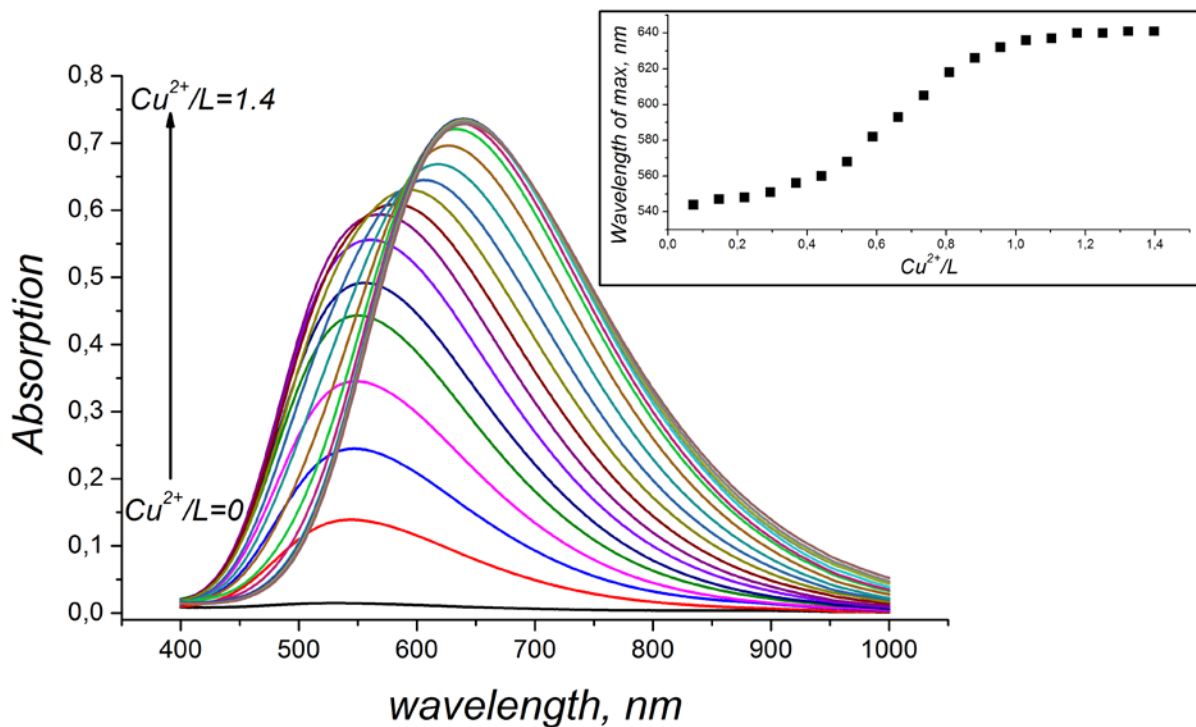


Figure S21. Evolution of absorption spectra upon addition of Cu^{2+} and absorption maximum shift with Cu^{2+}/L variation (inset), $\text{L}=\mathbf{1c}$

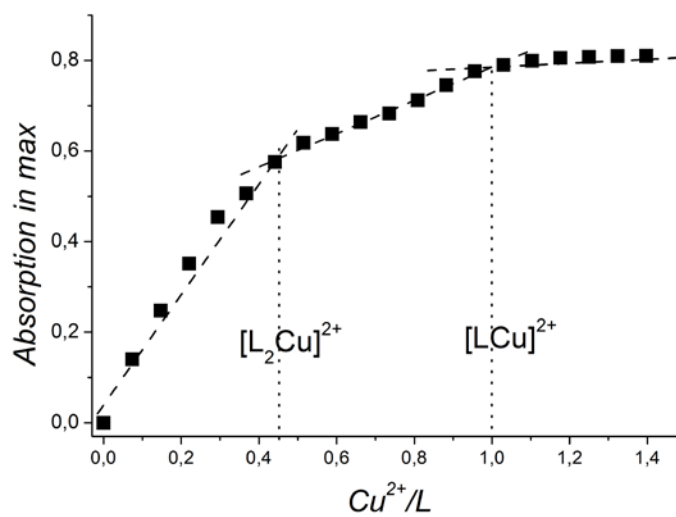


Figure S22. Absorption maximum shift with Cu^{2+}/L variation, $\text{L}=\mathbf{1c}$

NMR spectra

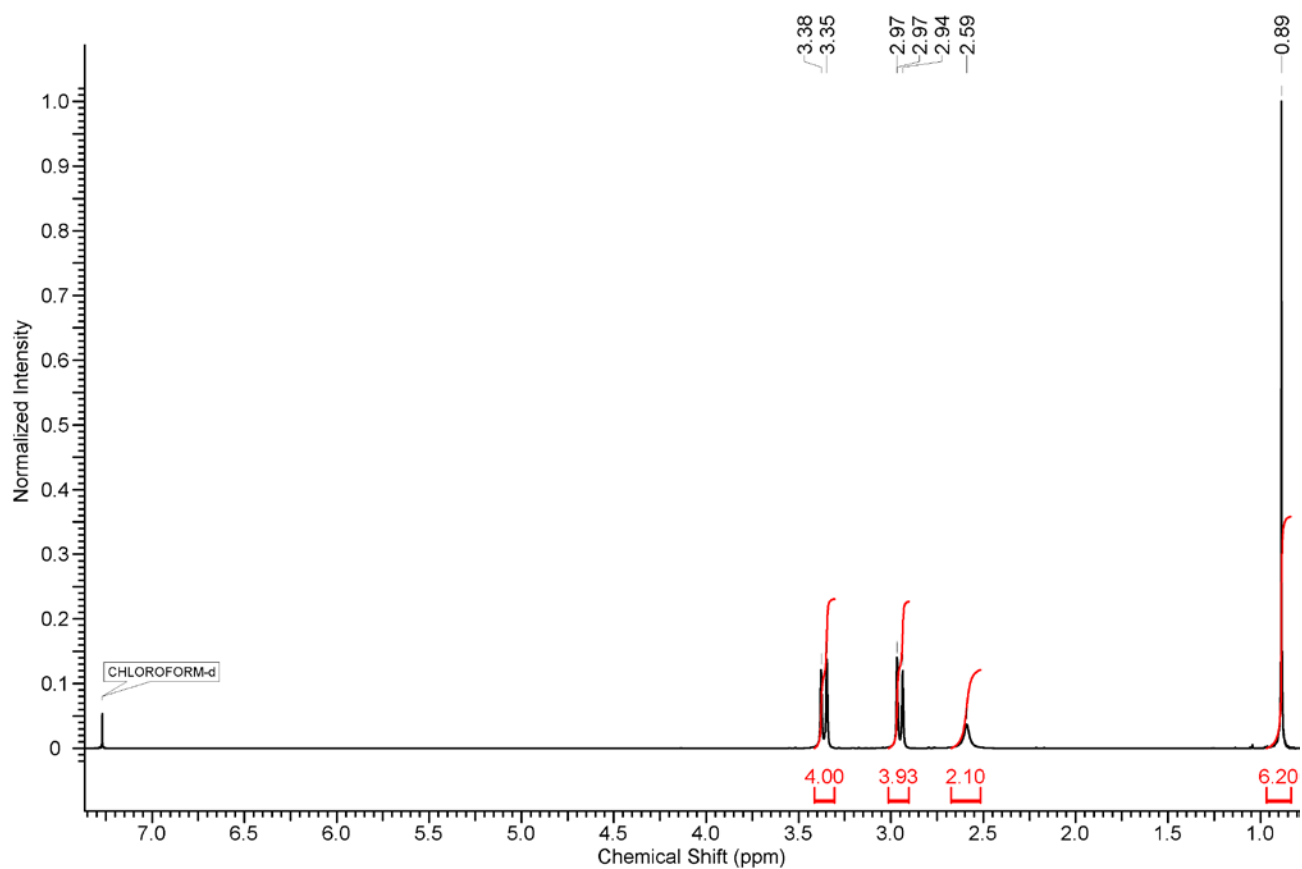


Figure S23. ¹H-NMR spectrum of 1,5-dimethyl-9-oxo-3,7-diazabicyclo[3.3.1]nonane (**1b**) in chloroform-d₁.

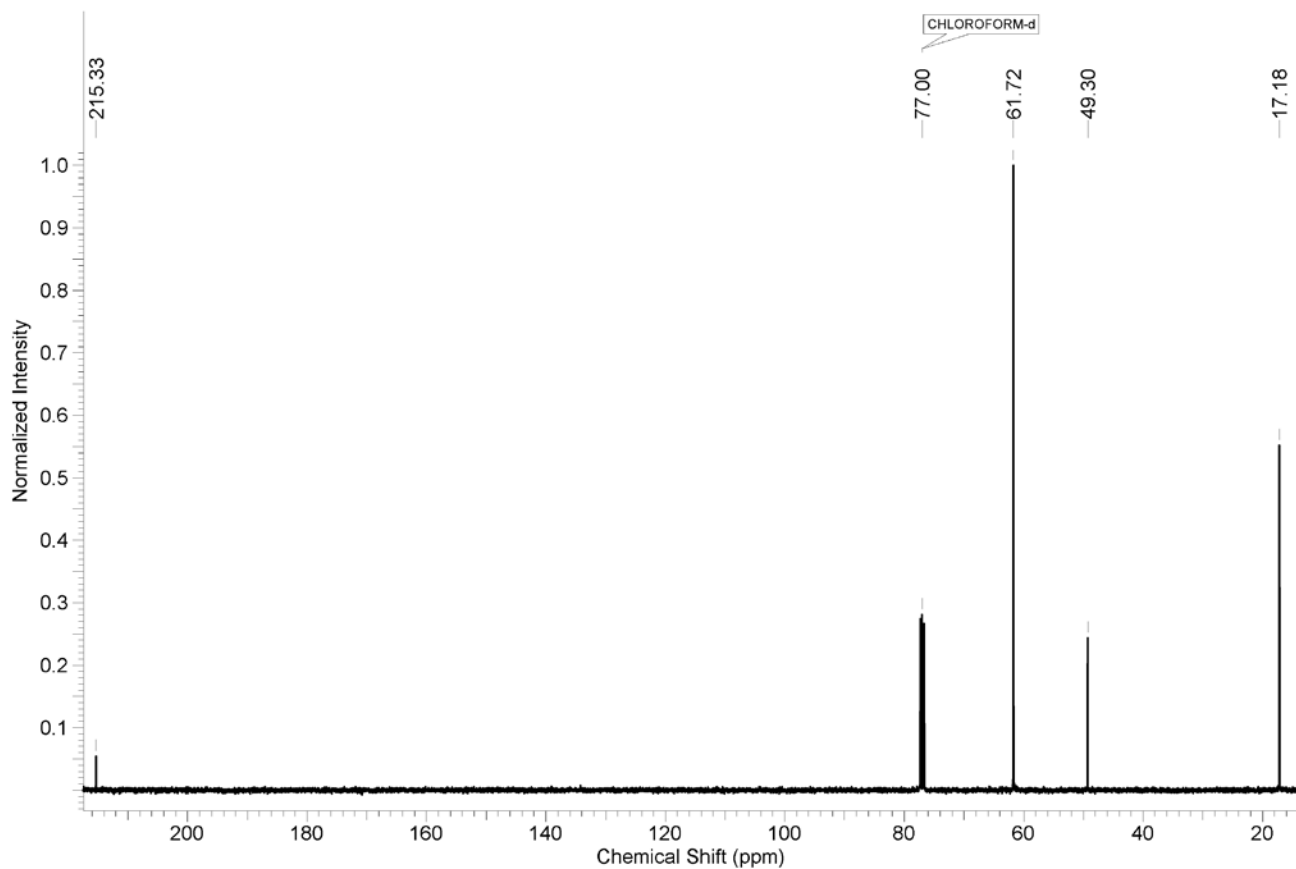


Figure S24. ^{13}C -NMR spectrum of 1,5-dimethyl-9-oxo-3,7-diazabicyclo[3.3.1]nonane (**1b**) in chloroform-d1.

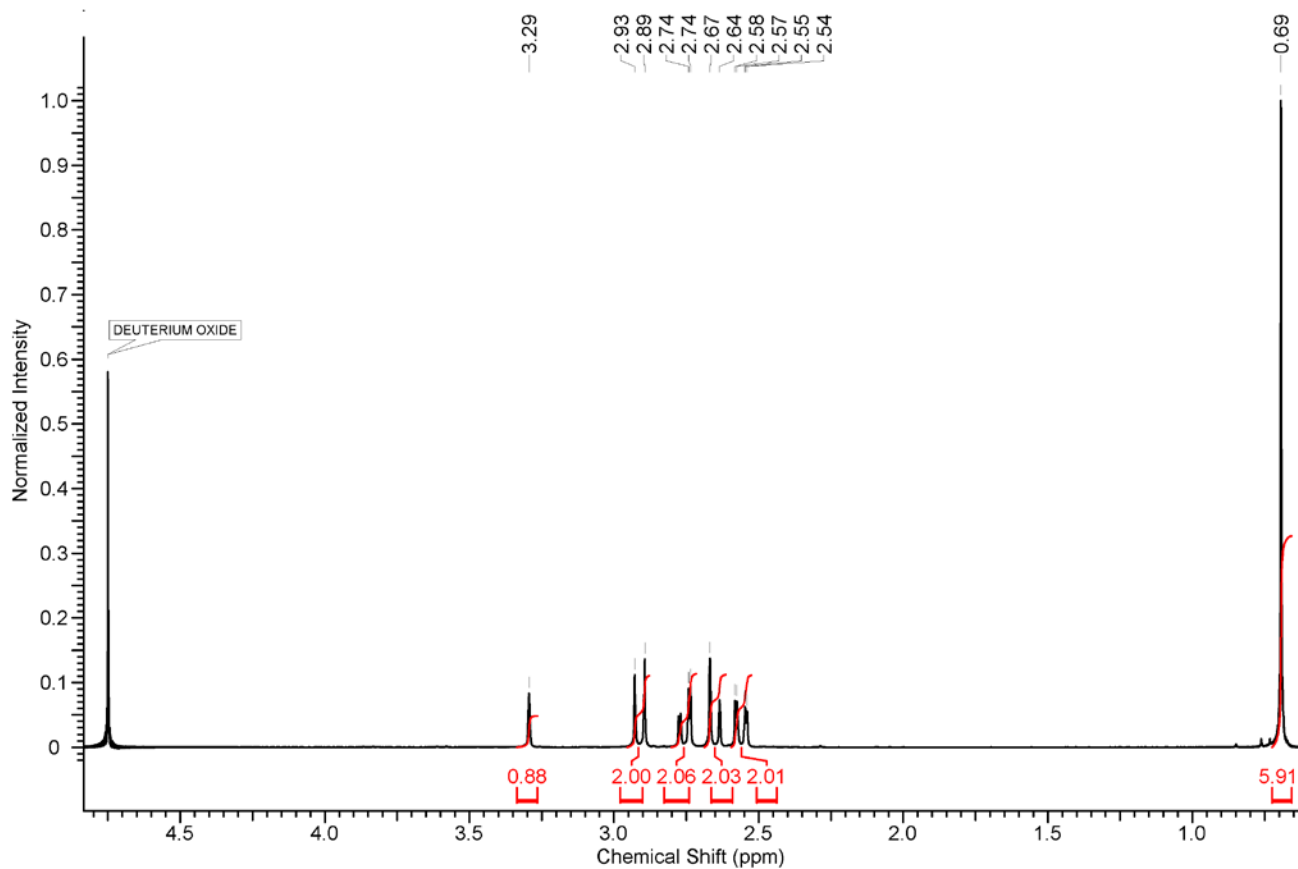


Figure S25. $^1\text{H-NMR}$ spectrum of 1,5-dimethyl-9-hydroxy-3,7-diazabicyclo[3.3.1]nonane (**1c**) in water- d_2 .

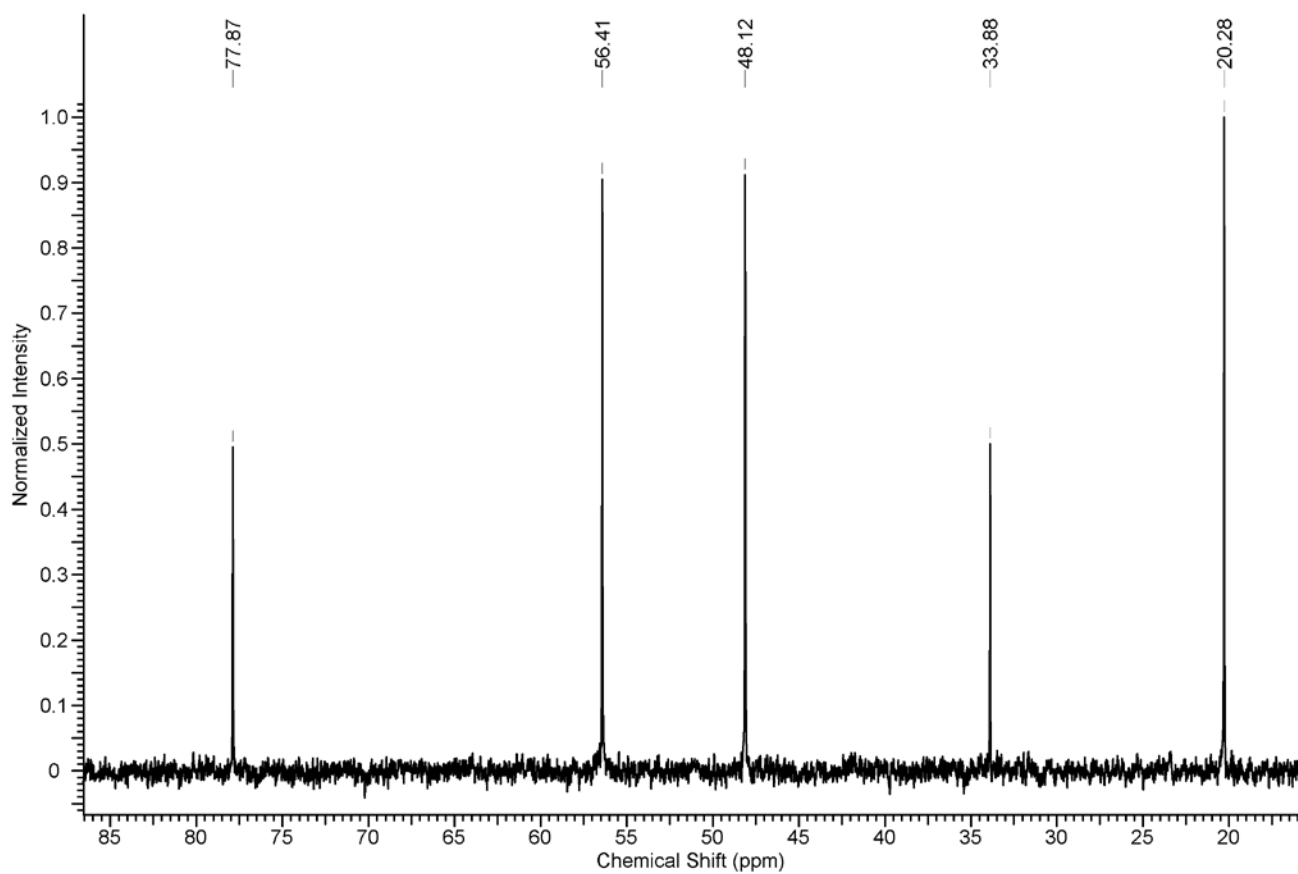


Figure S26. ^{13}C -NMR spectrum of 1,5-dimethyl-9-hydroxy-3,7-diazabicyclo[3.3.1]nonane (**1c**) in water- d_2 .

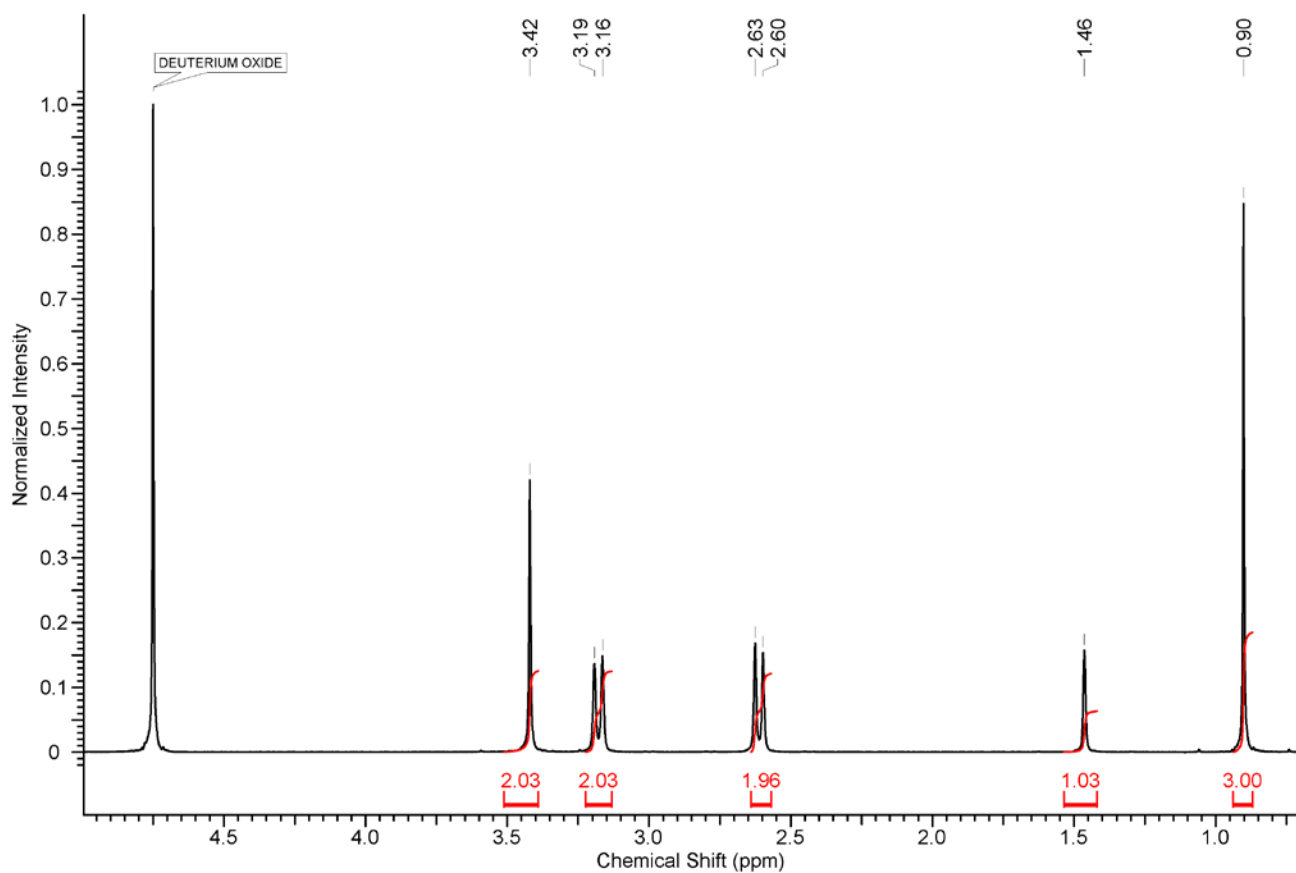


Figure S27. ¹H-NMR spectrum of 2,2'-(1,5-dimethyl-3,7-diazabicyclo[3.3.1]nonane-3,7-diyl)diacetic acid (**2a**) in water-d₂.

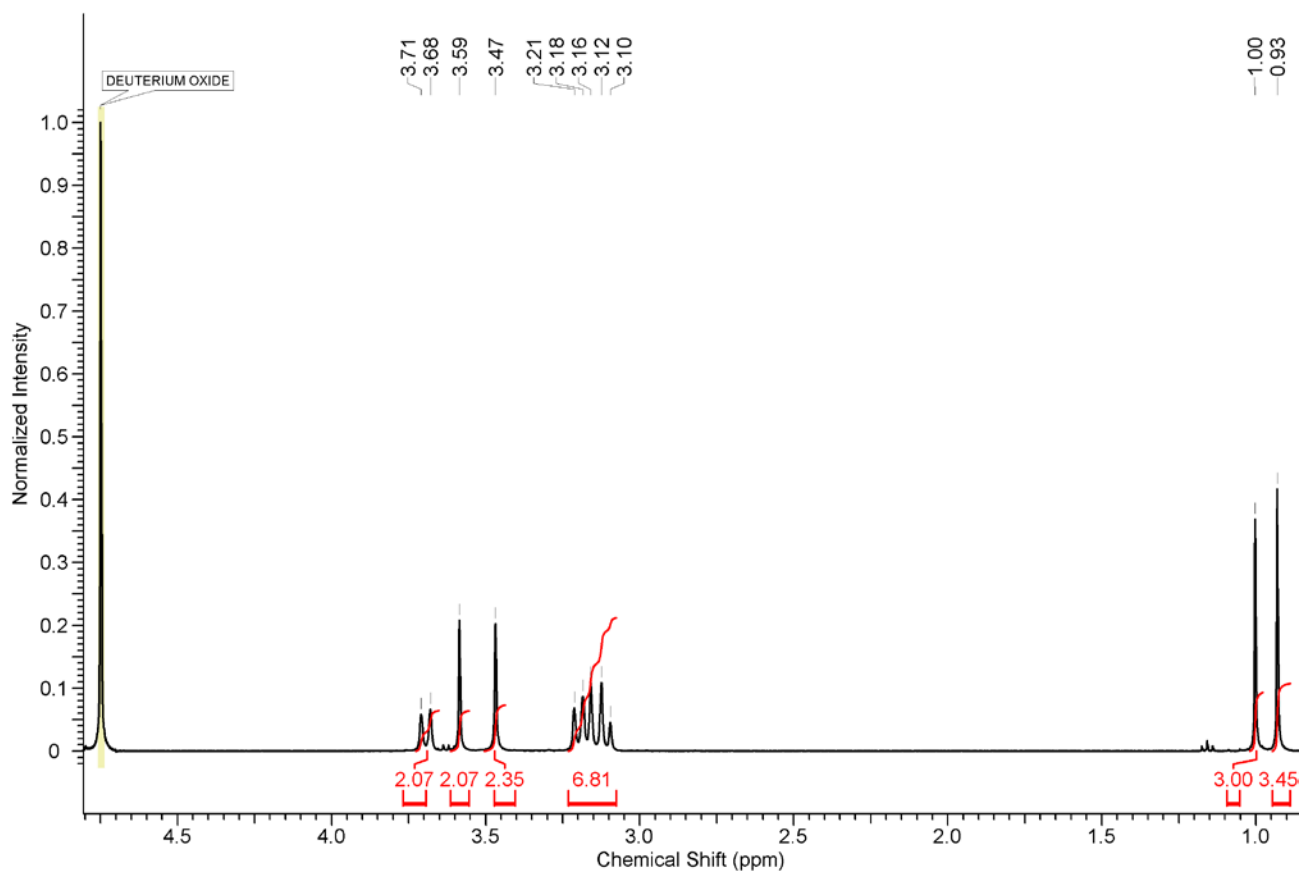


Figure S28. $^1\text{H-NMR}$ spectrum of 2,2'-(1,5-dimethyl-9-oxo-3,7-diazabicyclo[3.3.1]nonane-3,7-diyl)diacetic acid (**2b**) in water- d_2 .

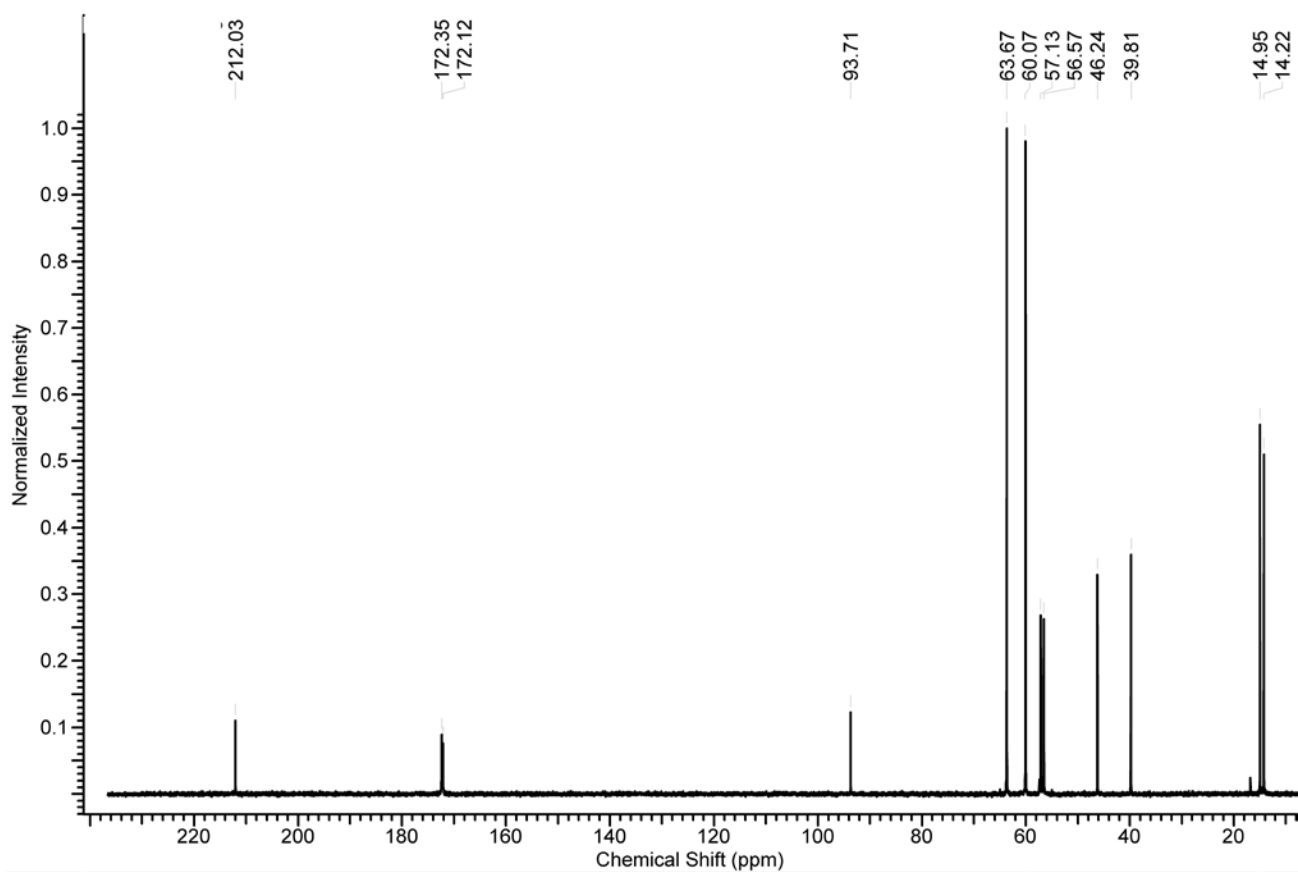


Figure S29. ^{13}C -NMR spectrum of 2,2'-(1,5-dimethyl-9-oxo-3,7-diazabicyclo[3.3.1]nonane-3,7-diyl)diacetic acid (**2b**) in water- d_2 .

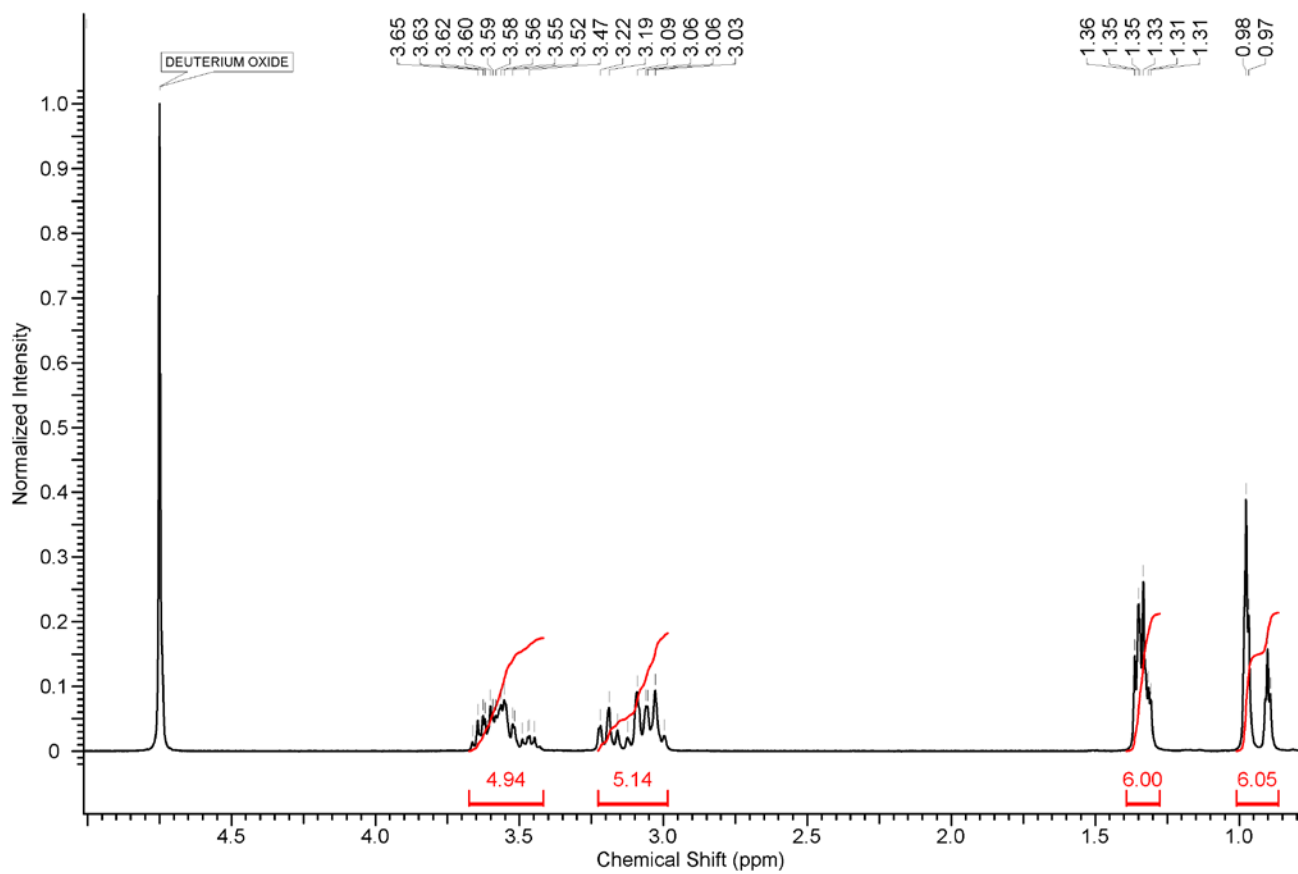


Figure S30. $^1\text{H-NMR}$ spectrum of 2,2'-(1,5-dimethyl-9-oxo-3,7-diazabicyclo[3.3.1]nonane-3,7-diyl)dipropionic acid (**3b**) in water- d_2 .

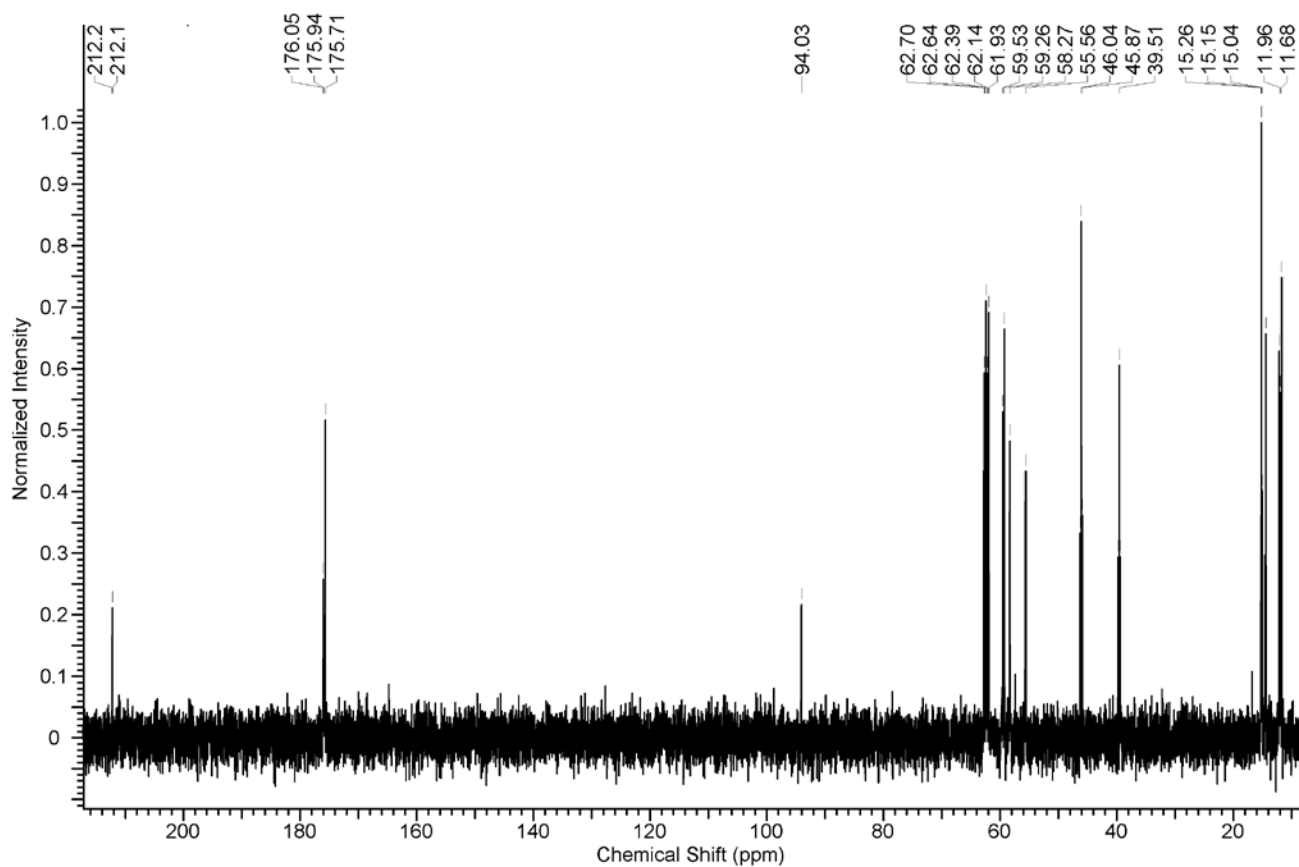


Figure S31. ^{13}C -NMR spectrum of 2,2'-(1,5-dimethyl-9-oxo-3,7-diazabicyclo[3.3.1]nonane-3,7-diyl)dipropionic acid (**3b**) in water- d_2 .

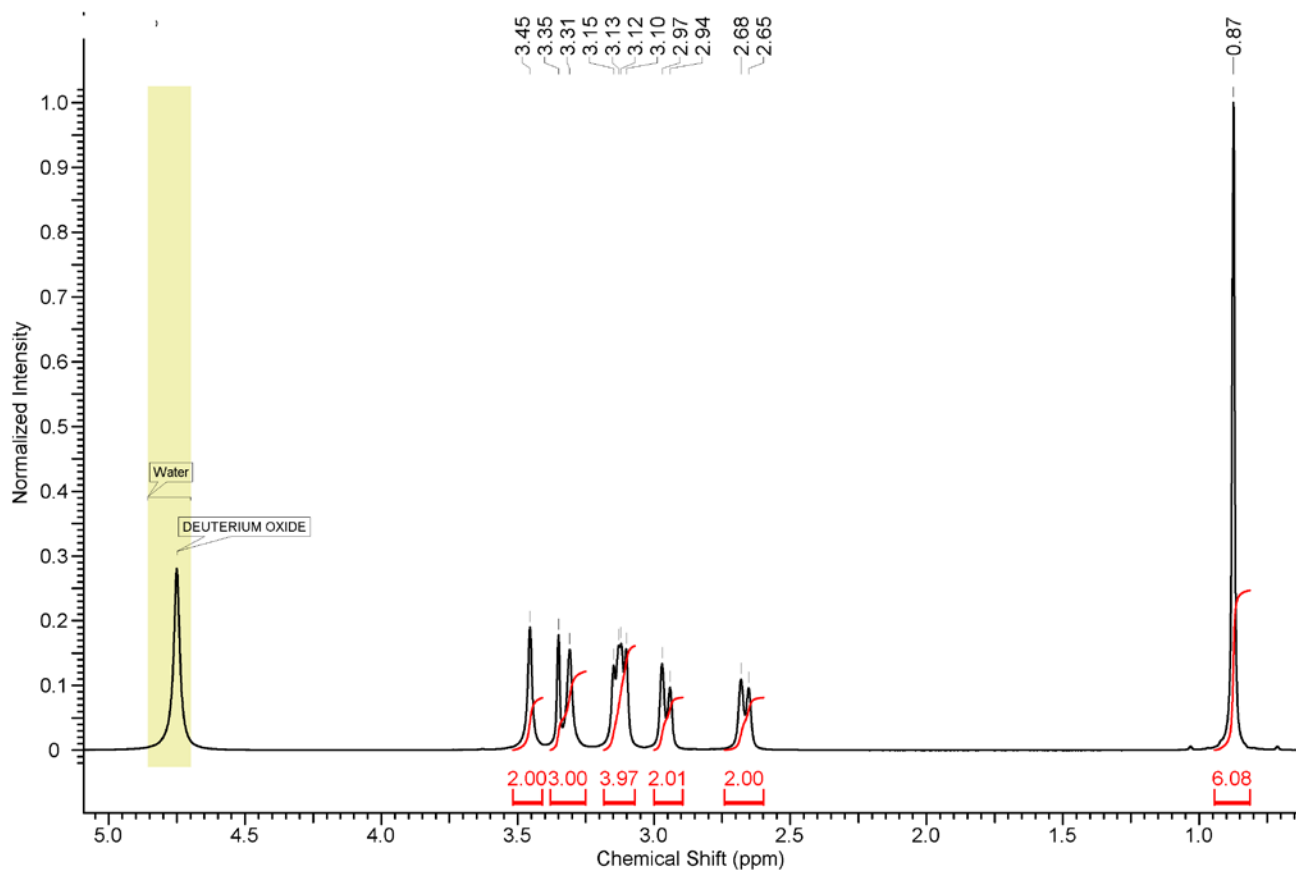


Figure S32. $^1\text{H-NMR}$ spectrum of 2,2'-(1,5-dimethyl-9-hydroxy-3,7-diazabicyclo[3.3.1]nonane-3,7-diyl)diacetic acid (**2c**) in water- d_2 .

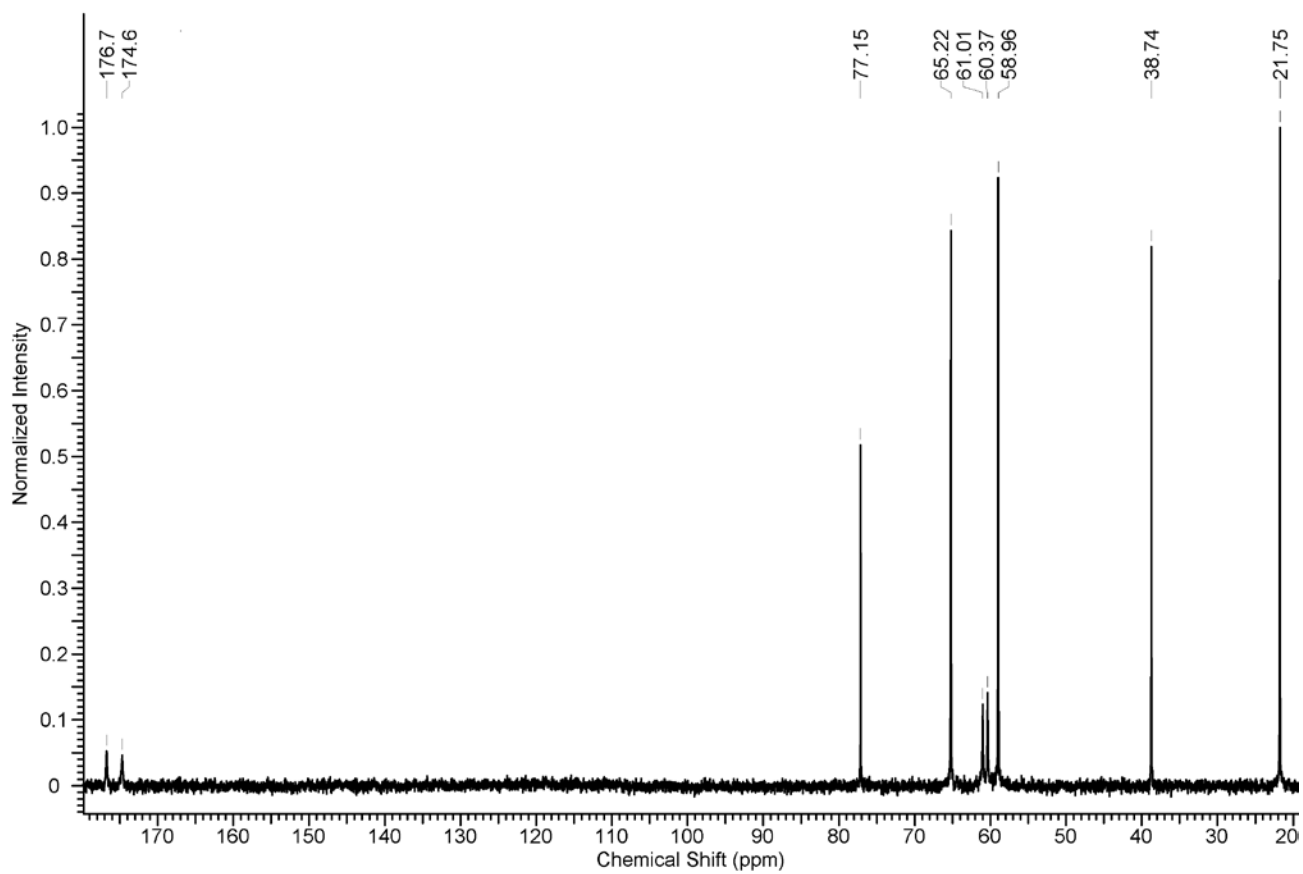


Figure S33. ^{13}C -NMR spectrum of 2,2'-(1,5-dimethyl-9-hydroxy-3,7-diazabicyclo[3.3.1]nonane-3,7-diyl)diacetic acid (**2c**) in water- d_2 .

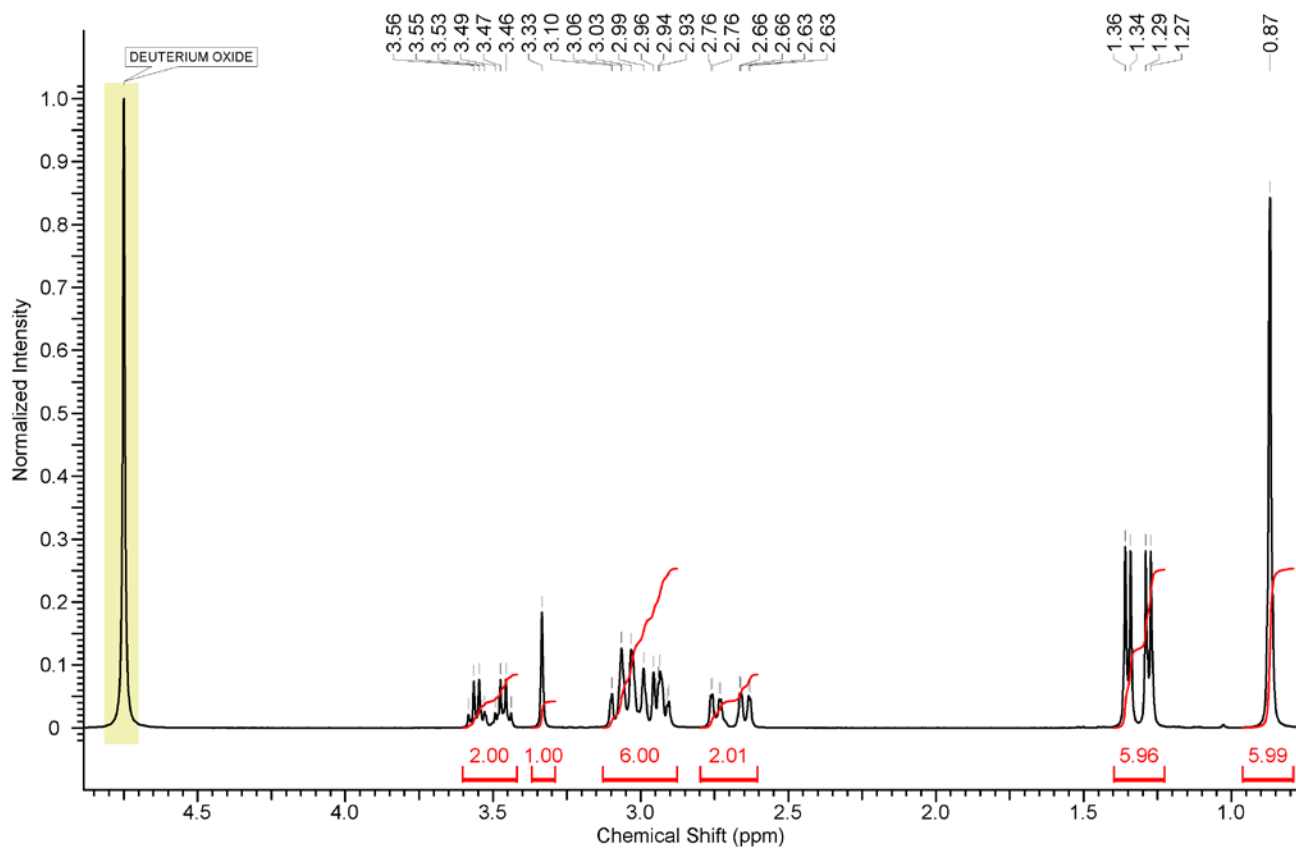


Figure S34. ^1H -NMR spectrum of 2,2'-(1,5-dimethyl-9-hydroxy-3,7-diazabicyclo[3.3.1]nonane-3,7-diyl)dipropionic acid (**3c**) in water- d_2 .

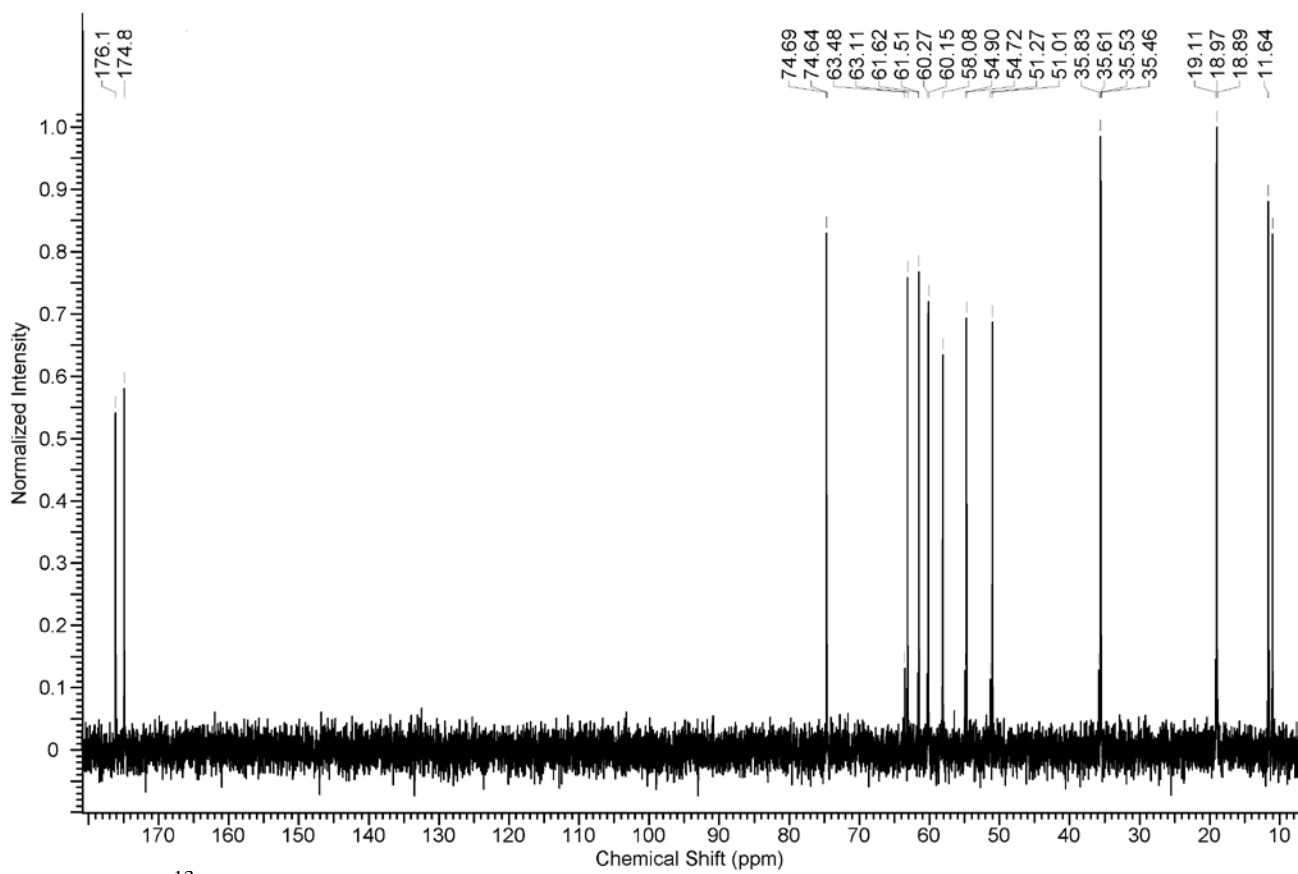


Figure S35. ^{13}C -NMR spectrum of 2,2'-(1,5-dimethyl-9-hydroxy-3,7-diazabicyclo[3.3.1]nonane-3,7-diyl)dipropionic acid (**3c**) in water- d_2 .

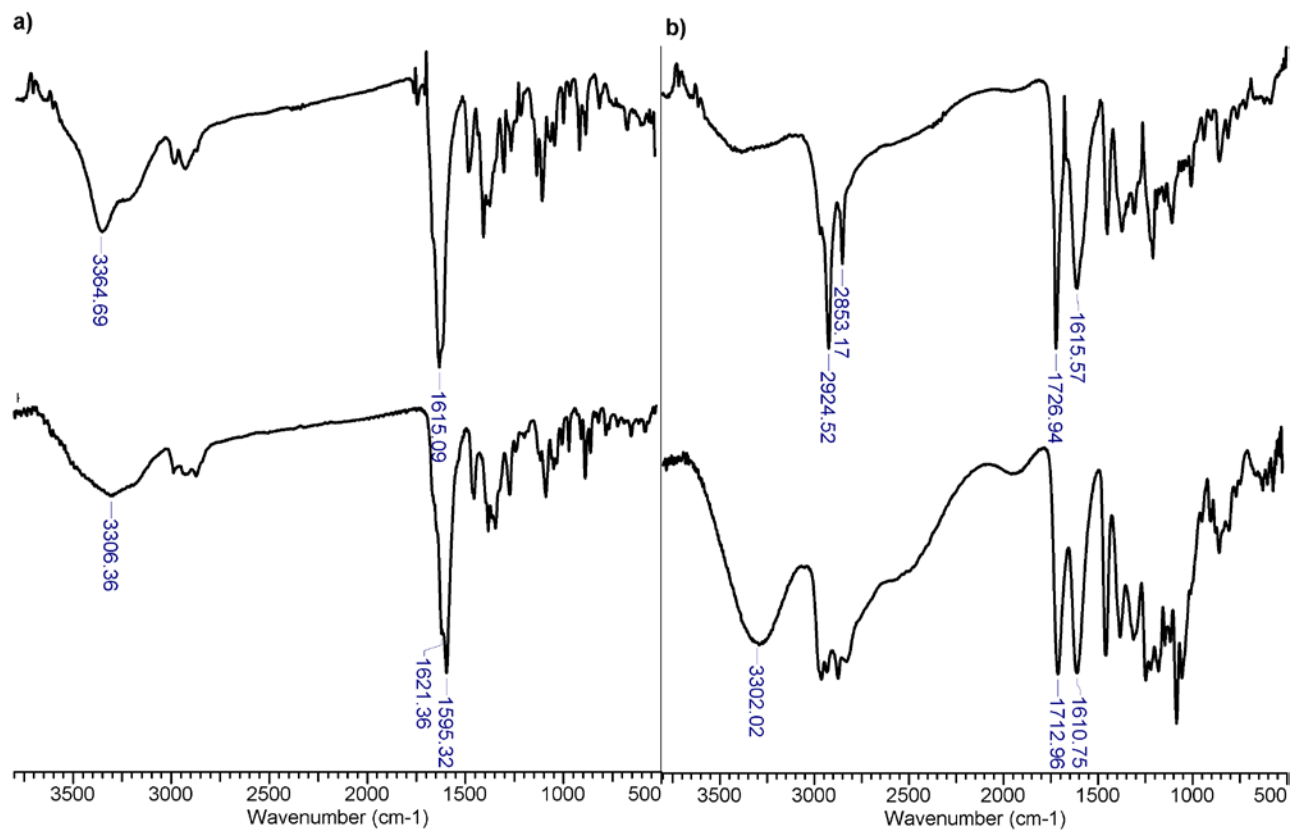


Figure S36. ATR-FTIR spectra of compounds **3b** and **5b** (a), **3c** and **5c** (b)

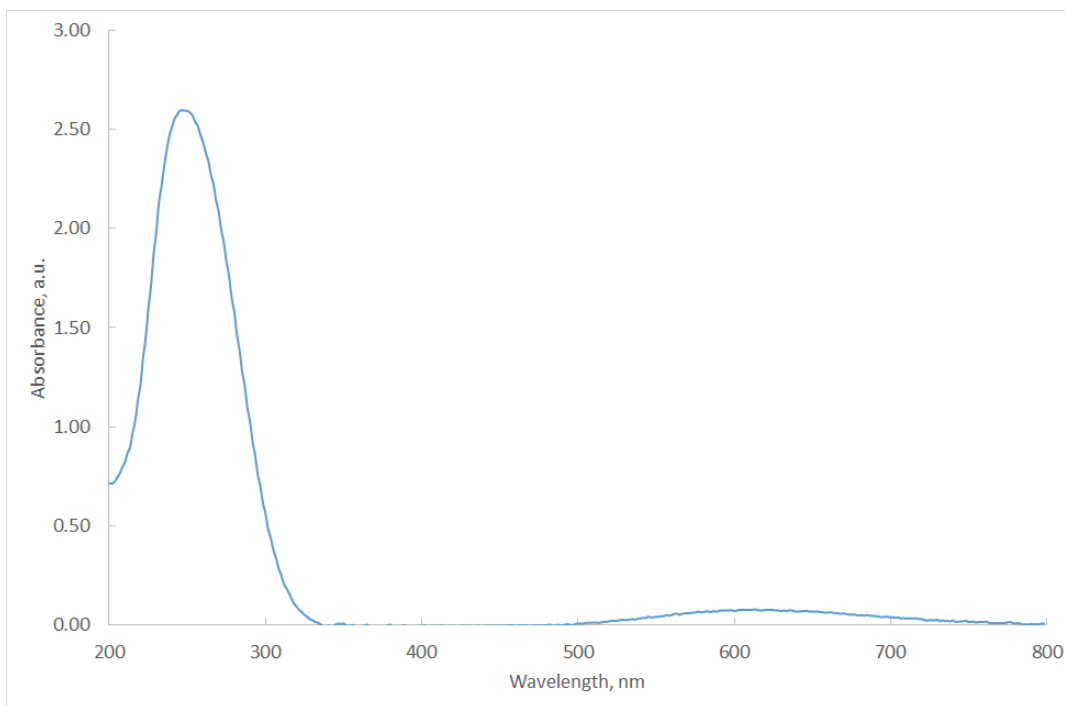


Figure S37. UV-vis spectrum of compound **4b** in methanol:water 1:1 solution. Concentration $5.34 \cdot 10^{-4}$ mol/l.

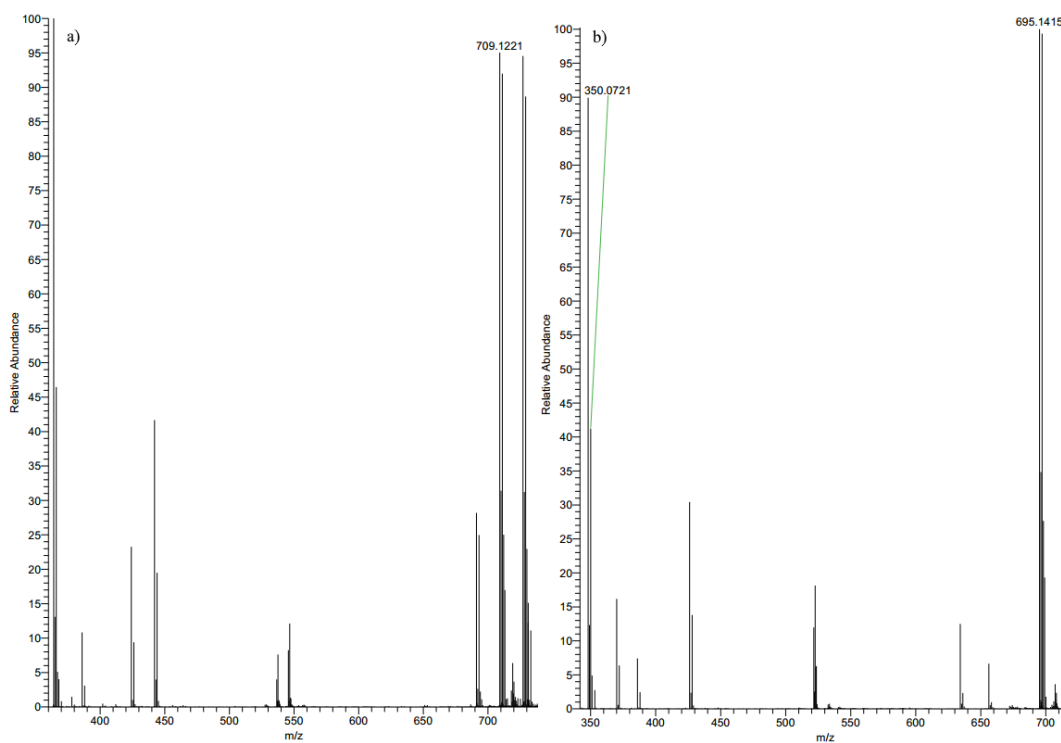


Figure S38. HRMS-ESI of copper complexes **4b** (a) and **4c** (b).

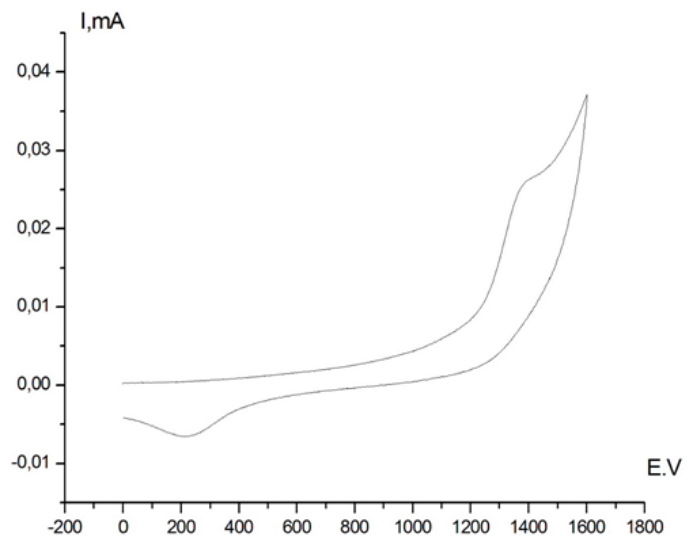


Figure S39. Cyclic voltammogram oxidation of complex **4c** (Pt electrode, DMF, Bu_4NBF_4 , $\text{Ag}/\text{AgCl}/\text{KCl}$ (sat.), $20\text{ }^\circ\text{C}$)

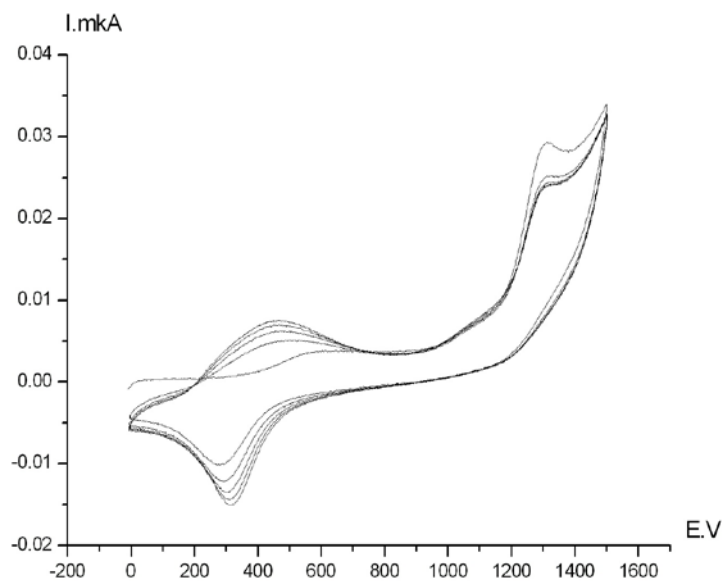


Figure S40. Cyclic voltammogram oxidation of complex **5c** (5 scan potential) (Pt electrode, DMF, Bu_4NBF_4 , $\text{Ag}/\text{AgCl}/\text{KCl}$ (sat.), $20\text{ }^\circ\text{C}$)